COASTAL MODEL PERFORMANCE

EVALUATION AND COMPARISON

Germana Peggion
Institute of Marine Sciences
The University of Southern Mississippi
Building 1103 Room 249
Stennis Space Center, MS, 39529
peggion@coam.usm.edu
phone: (601)-688-2897
fax: (601)-688-7072

MAY 97

ABSTRACT

Several ocean circulation models are evaluated and compared on coastal applications. The models are all primitive equation, free-surface models, that offer a wide range of mathematical and numerical formulations.

Two potential problem areas have previously been identified with the type of the compared ocean models: the use of σ-coordinates in steep bathymetry and unrealistically high dissipation that may prevent the formation of high gradient regions, simulation of small-scale features, and the proper onset of dynamic instabilities. A principal focus of this research is to evaluate the degree to which these problems limit the performance of the models in coastal applications. The model comparison is conducted over a series of experiments on semi-idealized configurations.

This study indicates that the solutions may sensibly differ from model to model. This is primarily due to: 1) different response to the calibration of the physical and numerical parameters, 2) perturbations in the dynamical balances. In general, differences in the primary features (such as front location, strength of the coastal jet) can be adjusted by adequate calibrations. Representation of the secondary features (such as internal wave propagation, temperature and salinity anomalies) may depend upon different parameterizations and numerical treatments of the same physical terms that may alter the relative importance of the dominant processes.

GOALS

The long-term goal is to contribute to the development of ocean predictive systems to support Naval operations in coastal areas. To date, the predictive capability in shallow water has not been addressed vigorously, and several aspects are still unresolved. This research will support the choice of the 'most suitable and accurate' model formulations to be applied in operational applications over the littoral areas.

OBJECTIVES

The objectives are to evaluate several ocean circulation models configured on limited-area coastal domains, compare the physical and numerical formulations, and prepare a series of guidelines and recommendations.

IMPACT

With the shift of the Navy's environmental interests from deep water to coastal regions, there is the need to redirect modeling requirements. Quantities of importance to Naval coastal operations include water depth, current speed and direction, surf, waves and swell, thermal and salinity structure, and water clarity. This study primarily focuses on the prediction of water depth, current speed and direction, and the evolution of the thermal and salinity fields.

1. INTRODUCTION

In past years, the Navy's primary ocean modeling efforts have been focused on developing global or basin-wide 3-D, eddy-resolving ocean circulation models. With the shift of the Navy's environmental interests from deep water to coastal regions, there is the need to redirect modeling requirements. It is recognized that coastal dynamics is physically quite different from the deep ocean. For example, typical time scales over the shelf are generally much shorter than on deep waters. Thus, prediction on coastal regions requires a different approach than forecasting at basin scale.

It is important to separate the physical regimes that can be realistically modeled, from those for which the model formulations are unsuitable. Test experiments are needed to compare model performances and evaluate the accuracy of the solutions. Quantities of importance to Naval coastal operations include water depth, current speed and direction, surf, waves and swell, thermal and salinity structure, and water clarity. This research will primarly focus on the prediction of water depth, current speed and direction, and the evolution of the thermal and salinity fields.

The approach is to compare existing ocean models in limited-area, coastal applications. Four free-surface, primitive equation models have been selected for the comparison:

- the Princeton Ocean Model (POM, Mellor and Blumberg),
- the Sigma Z-level Model (SZM, Martin),
- the S-Coordinate Rutgers University Model (SCRUM, Song and Haidvogel),
- the Estaurine Coastal Ocean Model Semi-Implicit (ECOMSI) (Blumberg).

The models offer a wide range of physical formulations (such as lateral and vertical mixing), and numerical algorithms (such as spatial and temporal schemes, implicit/explicit treatment of the barotropic flow) (Tab 1.).

Model comparisons offer a number of benefits and, to some degree, support the choice of the "most suitable and accurate" model to be transferred to operational applications, while sheding light on its forecasting skills. The comparisons can demonstrate the superiority of particular model formulations, model parameterizations, and numerical techniques. The scatter of the results from models that have been determined to be adequately and correctly formulated may provide an indication of the degree of uncertainity to be expected in the model predictions. Features that have been found to be particularly efficient and/or accurate can be extracted from one model and incorporated in

another.

If two model solutions are significantly different, the differences can be examined to determine why the models differ, and which model is most likely to be *correct*. If models agree, it does not, guarantee that they are both correct, but it does increase our confidence in the results.

The physical accuracy and the numerical character of the models are evaluated on a variety of test problems. The coastal study processes include 1) wave propagation, 2) upwelling and downwelling regimes, 3) set up of wind driven circulation, and 4) genesis and evolution of fronts instabilities.

2. MODEL ASSESSMENTS

The models have generally been retrieved by anonymous ftp. With the exception of SCRUM, the programs were usually condensed in one or two file. That made it difficult to isolated parts of the codes or verify parameter values. Therefore, all the models have been configured on a modular form and compiled through the 'make' command. Following SCRUM's model architecture, C-preprocessor derectives were included in the F77 programs. This allows one to conditionally include part of the code before the F77 compile sees them, to save the expense of compiling and linking options that are not being used in a given model configuration, and to add/bypass parts of the code with minimum changes in the programs. The modifications have increased the models' portability on several platforms, and reduced the compiling process when only a few changes were made in a model's configuration.

All the models were also linked to the plotting package developed by K. Hedstrom at Rutgers University, which makes use of the NCAR Graphic software. This made it possible to visually compare model solutions on a common ground for a more stringent evaluation. Since the variability of the model's solutions is one of the major topics of the comparison, the output has been interfaced with the Empirical Orthogonal Functions (EOF) programs developed by D. Fox at NRL and recently implemented at COAM.

The models are configured with idealized geometries and with sufficient horizontal and vertical resolution to provide accurate estimates of the dynamics. All the tests are confgured on a periodic channel to avoid the application of open boundary algorithms that could have altered the model evaluation and comparison.

3. ROBUSTNESS

One issue addressed is to determine the robustness and portability of the models. Simulations investigate how and if mixing algorithms, filtering and smoothing procedures contribute to the models' numerical stability at the expenses of the physical accuracy.

3.1 The Choice of the Vertical Coordinate

The choice of the vertical coordinate transformation is a controversial and unresolved issue. The z-levels have the flexibility of a high resolution near the surface, for a good representation of the Mixed Layer (ML) dynamics, and a coarser resolution in the deeper strata, so that they are numerically efficient. However, since the bathymetry is approximated by a step-like function, topographic effects may be poorly parameterized (Martin,1997 manuscript in preparation).

A series of problems have been recognized and documented for the σ-coordinates. The pressure forces and vertical advection terms may be affected by the computer truncated arithmetic, with sensible loss of accuracy and stability. For n evenly-spaced σ-levels, the hydrostatic consistency is defined by the ratio:

$$r = \frac{1}{nH}\frac{\Delta H}{\Delta x}$$

(Mellor et al.,1994; J. Atm. and Ocean. Tech.). Although the problem may become severe in coarse grid resolution with steep topography or/and strong stratification, the topography gradient and the numerical grid resolution for most of the coastal applications satisfy the hydrostatic consistency condition.

3.2. The Implicit and Explicit Formulations

It is well known that implicit schemes are less accurate, but more efficient than the explicit schemes (Grotjan and O'Brien, 1976; Mon. Weath. Rev.). Explicit schemes are always more accurate in wave propagation and energy trasport, even for those waves that are solved by several grid points. Implicit schemes retain stability by slowing down the traveling features.

There is a fundamental difference between implicit and explicit treatment of the barotropic flow. Explicit schemes have a local character: at any grid point the solution is updated

by knowledge of the fields at the previous time steps and closest surrounding points. On the other hand, implicit schemes depend upon the application of algorithms for the solution of 2-D elliptic equations, which present a global character: the field is obtained by solving simoultaneously an algebraic set of equations that connects points geographycally distant.

3.2.1. The Truncation error

Elliptic solvers usually rely on iterative methods and a compromise has always to be found between accuracy and computational cost. Experiments evaluate how the barotropic flow is affected by the choice of the truncation error in an iterative procedure. The tests are conducted with the SZM model which includes the Simuoulaneous Over-Relaxation (SOR) cyclic boundary algorithm. Although the SOR procedure is most likely to not be used in realistic coastal applications, it makes evident problems that it may share with other more sophisticated algorithms. The simulations analyze the response to a longshore wind forcing of a stratified channel with an uniform along-channel bathymetry, so that the problem is truly 2-D. The sea surface mean values appear to be a good indicator as to whether or not the solver has reached a reasonable accuracy. The physical problem conserves the initial mass, but the computed mean surface values are roughly of the same order of magnitude of the specified truncation error after 1 day of simulations. Although differences in the velocity values are within errors of few millimeters per second, the cumulative truncation error may sensibly change the current systems over extended simulations.

3.2.2. The correction procedure

The presence of the nonlinear terms in the barotropic flow equations implies terms such as $h^{n+1}u^{n+1}$ that complicate the application of the implicit schemes. In general, the advective terms are approximated by $h^{n}u^{n+1}$, in order to avoid the solution of a nonlinear differential equation. However, the formulation may lead to inconsistencies of the numerical algorithm.

SZM introduces an iterative procedure to correct the advection terms of the momentum equations. It is found that the correction procedure increases the accuracy of the semi-implicit formulation. At the second corrective iteration, the number of the SOR's iterations may range from 20 to 30% of the previous passage, indicating that at least

two passages are necessary to achieve a higher convergence of the elliptic solver, and a higher consistency of the implicit scheme.

Although the simulations support the usefulness of a corrective algoritm, the procedure is neglected in most of the free-surface, semi-implicit models. The weakness of the SZM approach is the computational cost, since the corrective iterations are performed over the 2-D and 3-D fields. It would be important to verify the efficiency and accuracy of a corrective procedure applied to the external mode only.

3.3. Time Filtering

Both POM and SZM make use of the Asselin filter to avoid the splitting modes of the leapfrog scheme. As Appendix A illustrates, the Asselin filter is diffusive, Consider a wave that travels one grid spacing over μ time iterations, such that $C = \Delta x/(\mu \Delta t)$. For the values Δx =7.5 km, Δt = 900 s, and the typical Asselin parameter a= 0.05, the diffusive coefficient of (A.5) is: $N_c \sim 1500/\mu^2$

i) slow waves : μ = 10 $N_c \sim$ 9 $m^2 s^{-1}$

ii) fast waves : μ = 2 $N_c \sim$450 $m^2 s^{-1}$

For slowly-varying (with respect to the time increment) features, time splitting is not a severe problem and generally, the computational mode does not amplify to critical levels (Mesinger and Arakawa, 1976; GARP Series, 17), and the Asselin filter may not be an essential component for the model stability. However, for the fast waves, the computational eddy coefficient of the Asselin filter may became sensibly greater than the average value of the Smagorinsky coefficients, and the algorithm may alter the dominant dynamical balances of the fast traveling features.

3.4. Horizontal Diffusion

One of the common potential problems for σ-coordinate models is the application of the horizontal diffusion operator acting on surfaces of constant sigma. The numerical formulation is an approximation of the diffusion operator on the σ-transformation and might generate computational heating/cooling sources in regions of steep topography. Experiments evaluate the physical accuracy and computational efficiency of the geopotential diffusion operator introduced by Barnier et al. (1996, Deep Sea Res.). As Fig. 1. illustrates the rotation of the tensor eliminates the spurious heating in the proximity of the

continental break and shelf. The new algorithm sensibly reduces the across-channel gradient in the constituent fields at the shelf break.

3.5. Hybrid Numerical Schemes

The early versions of the SCRUM model (henceforth referred as SCRUM_1) were designed with hybrid schemes, such as II order finite differencing for the horizontal, and I order finite element for the vertical derivative terms. In this configuration, the model did not performe at the expected level. The newest version of the SCRUM model (henceforth referred as SCRUM_2) has removed the vertical finite-element formulation and substituted it with the classical II order finite differencing, and the models' preformance has improved tremendously. This may suggest that it is important that terms that are dynamically in balance be numerically treated with schemes at least with the same truncation errors. Unfortunately, SCRUM_2 has been released toward the end of this project and has been tested in only few cases.

4. MODEL COMPARISON

4.1. Wave Propagation

Waves are an essential component of coastal dynamics and provide an useful test problem for model evaluation. The classic freely propagating linear waves are analyzed: barotropic shelf waves (BW), Kelvin (KW) and Poincare waves (PW). For those, an analytical solution is known in the rigid lid (BW) and small amplitude (KW and PW) approximations. The model accuracy is determined by the correlation factor and rms error (in percent) between the numerical and analytical solutions. The goals of the experiments are twofold: they seek 1) to determine the accuracy of the solutions as a function of number of grid points per wavelength and 2) to analyze how advection and mixing terms may distort the propagation of the free waves. Thus, the experiments are configured also as a function of the Rossby number $\epsilon = UL/\mathrm{f}$. Henceforth, the term linear refers to simulations in which the wave amplitude has been specified to keep the Rossby number small.

All the models show high correlation factors between the analytical and numerical solutions for the linear waves solved by several grid points. The correlation factor decreases as the number of grid points per wavelength is reduced. As the number of grid point per wavelenght is reduced or the Rossby number is increased, the correlation factors de-

crease rapidly for all the models, but without sensible differences among the models' performance.

4.2. Long-term Wind Driven Circulation

The tests analyze the response to an along-shore wind on a periodic channel. The channel is 377 km wide and 535 km long. The shelf-break is parabolically shaped. The shallow region (30 m depth) is 30 km wide at the middle channel and 100 km at the boundaries. The maximum depth is 300 m and the mean bathymetry gradient is 0.005. The wind stress (1.2 $m^2 s^{-2}$) is steady and uniform in the along-shore direction and set to zero in the deep part of the channel with a cos-like function.

4.2.1 Downwelling

POM generates the smoothest and weakest coastal jet. The maximum along-channel velocities are at the shelf break and the coastal jet extends well over the whole continental slope. SZM's coastal jet is narrower and located more offshore, with the axis in the deepest part of the continental slope. The coastal current system of SCRUM_1 solution is located further offshore, and it is generally wider than in the other models. SCRUM_1 also produces the highest horizontal velocities values among the solutions. However, the strong currents are confined on a thin surface layer. Moreover, SCRUM_1 develops sub-scale, noisy features at the middle and bottom depth of the water columns. Tab. 2. summarizes and compares the model solutions

The across-channel velocities also have distinct features. At the vertex of the parabolic-shaped shelf, the cross-channel velocities break into in- and off-shore translations that are associated with areas of strong up/downwelling that affect the whole water column over the continental slope. Comparison of the model solutions indicates that there is no apparent correlation among the sub-scale features generated by each model.

Fig. 2a compares the distribution of the temperature and salinity fields at the middle cross section. Values are approximately about 7.5 m below the surface. POM and SZM temperature surface values exceed the maximum initial value over the shelf and shelf break due to the treatment of the lateral mixing operator (see Sect. 3.4.). SCRUM_1 does not present evidence of unrealistic overheating, and the surface temperature is the coolest among the models.

4.2.2. Upwelling

POM's coastal jet is wider and located at the mid-continental slope; the mesoscale activity is mainly confined in the upper water column and generates at the offshore edge of the current system. At the inner edge, near-bottom currents develop close to the shelf-break, carrying bottom water over the shallow shelf. SZM's coastal jet is narrower and located over the deepest part of the continental slope; mesoscale eddies and meandering are visible over the whole wind-forced deep region. Similarly to the downwelling case, the cross-channel velocity breaks into in/offshore translations at the shelf middle point and no significant correlations are found between the model solutions. The models produce marked differences also in the constituent fields and mixed layer configuration. Fig. 2b. compares the near-surface temperature and salinity distributions at the shelf's middle point. For all the models, near-bottom currents at the shelf break carry cold and salty water into the inner coastal region. With respect to the initial distribution, all models present surface temperature minimum and salinity maximum in the proximity of the shelf break, with a more marked horizontal gradient in the SZM and SCRUM_1 solutions that is associated with a stronger local upwelling regime. Over the continental slope, surface temperature increases steadly with distance from the coast. POM's initial surface values and stratification are recovered outside the wind-forced region. SCRUM_1's surface temperature values increase only sligthly over the deep part of the channel, indicating that the model is subjected to a stronger upwelling everywhere, probably trigged by the inconsistency of the advective schemes.

The evolution of the salinity field is consistent with the associated temperature distribution. The less marked differences between POM and SZM solutions are due to the initial constituent distributions for which salinity is homogeneous in the upper 30 m, while temperature is linearly stratified.

4.3. Internal Waves Under a Downwelling regime

These experiments analyze the genesis of internal waves as a function of the grid spacing. The problem is 1-D, i.e., the bathymetry is uniform in the along-shore direction and ranges from 20 to 200 m with a mean slope gradient of 0.001.

Figs 3a and 3b illustrate the solution at Day 45 for the grid spacing of 4 and 1 km, respectively. Long runs are conducted to verify the model stability. Tests are performed with

the old and new version of the SCRUM model. It is found that the new version increases dramatically the model solution and removes the sub-scale noise that characterized the early program. Figs 4a-c illustrate the EOF mode for the solution at days 12-15. All the models generate internal waves represented by the first 2 modes, that account for more than 50% of the total variability. The remaining energy is distributed among the higher mode differently. This is generally a consequence of the different algorithms used by the models for the treatment of the vertical mixing.

4.4. Genesis and Evolution of Front Instabilities.

The simulations reproduce the test-case illustrated in Wang (1993, J. Mar. Sci.). The problem is configured on a periodic channel. The initial condition represents a 2-D density front and the velocity derived by each model with diagnostic calculations. A small amplitude pertirbation is superimposed to the basic state. The disturbance starts growing and the cyclonic vorticity becomes so large that the wave crest is bent backward enclosing an isolated eddy (Fig. 5).

SCRUM_2 gives the more marked eddy. This is probably a consequence of the constant horizontal eddy coeficients (5 m^2s-1) that are equivalent to the mean, but also much smaller than the maximum values of the Smagorinsky coefficients. Since the Smagorinsky algorithm is a function of the velocity shear, SCRUM_2 is much less diffusive at the edge of the disturbance. On the other hand, SCRUM_2 is more diffusive than the other models in the lower region of the channel, and the front is smoothed at the warm side.

Tests are also performed to verify the sensitivity of the models to the specification of the vertical mixing algorithms, and to the vertical grid resolution.

5. CONCLUSIONS

This study compares several ocean circulation models in coastal applications. The comparison is restricted to 3-D, primitive equation, free-surface models on sigma-like vertical coordinate systems. The models differ in their treatment of the barotropic flow, horizontal and vertical mixing, temporal and spatial differencing, and other details. The physical accuracy and the numerical character of the models are evaluated and discussed on a variety of test problems. The coastal study processes include wave propagation, upwelling and downwelling regimes, and genesis and evolution of fronts.

One issue addressed is to determine the robustness and portability of the models. Simulations investigate how and if mixing algorithms, filtering and smoothing procedures contribute to the models' numerical stability at the expenses of the physical accuracy. One of the common potential problem areas is the application of the horizontal diffusion operator acting on surfaces of constant sigma. The formulation might generate computational heating/cooling sources in regions of steep topography.

The study indicates that the solutions may sensibly differ from model to model. This is primarily due to: 1) different response to the calibration of the physical and numerical parameters, 2) perturbations in the dynamical balances. In general, differences in the primary features (such as front location, strength of the coastal jet) can be adjusted by adequate calibrations. Representation of the secondary features (such as internal wave propagation, temperature and salinity anomalies) may depend upon different parameterizations and numerical treatments of the same physical terms that may alter the relative importance of the dominant processes.

APPENDIX. The Asselin Filter

Consider the advection equation:

$$u_t = Cu_x \tag{A.1a}$$

and the associated numerical approximation:

$$\frac{u^{n+1} - u^{n-1}}{2\Delta t} = C\frac{(u_{j+1} - u_{j-1})^n}{2\Delta x} = CD_x^n \tag{A.1b}$$

Deriving on time, eqs (A.1) are equivalent to:

$$u_{tt} = C^2 u_{xx} \tag{A.2a}$$

$$\frac{u^{n+1} - 2u^n + u^{n-1}}{\Delta t^2} = C^2\frac{(u_{j+1} - 2u_j + u_{j-1})^n}{\Delta x^2} = C^2 D_{xx}^n \tag{A.2b}$$

The Asselin filter is applied over two time steps:

1) compute u^{n+1} from eq (A.1b)
2) correct u^n : $u^n = u^n + a(u^{n+1} - 2u^n + u^{n-1})$

At the following time step, the variable u^{n+2} is computed from:

$$\frac{u^{n+2} - u^n}{2\Delta t} - \frac{a\Delta t}{2}\frac{u^{n+1} - 2u^n + u^{n-1}}{\Delta t^2} = CD_x^{n+1} + O(a) \tag{A.3}$$

From eq (A.2b) it follows:

$$\frac{u^{n+2} - u^n}{2\Delta t} = CD_x^{n+1} + \frac{a\Delta t}{2}C^2 D_{xx}^n + O(a) \tag{A.4}$$

Thus, similarly to other smoothing procedure, the Asselin filter is diffusive with a computational eddy viscosity coefficient:

$$N_c = \frac{a\Delta t}{2}C^2 \tag{A.5}$$

LIST OF TABLES

LIST OF FIGURES

Tab. 1. The model attributes

	POM	SZM	SCRUM	ECOMSI
h. coord	Bnd Fitt	Cart (dx=dy)	Bnd Fitt	Bnd Fitt
v. coord	σ	σ & z	s	σ
masking	y[1]	y[1]	y	y[1]
h. sch	F Diff	F Diff	F Diff[2]	F Diff
v. sch	F Diff	F Diff	F Elem	F Diff
Int mode	LpFr	LpFr	h. AdB v. SImp	Frwd
Ext mode	Time spl	Impl[3] & Expl	Time spl	Impl
Filter.	Y	Y	No	Y
h. mix	Smag	Reyn	Lapl[4] & Bih[4]	Smag
v. mix	MY2.5	MY2.0	PrPh & MY2.0	MY2.5
bot fric	quadr[5]	quadr[5]	linear & quadr[6]	quadr[5]

1) Masking used for closed boundary conditions
2) Option for forth order scheme on pressure forces.
3) conservation scheme applied
4) constant eddy coefficients.
5) drag coefficient as function of friction vel.
6) constant drag coefficients.

Tab. 2a. The Wind Driven Experiment: Downwelling

	30 d			60 d			90 d		
	Mn	Mx	Av	Mn	Mx	Av	Mn	Mx	Av
POM									
U	-1.02	0.04		-1.19	0.10		-1.05	0.11	
V	-0.32	0.46		-0.42	0.52		-0.38	0.53	
W*	-0.13	0.09		-0.26	0.30		-0.26	0.30	
η	-0.14	0.37		-0.17	0.43		-0.19	0.44	
KH	0.25*	14.79	588.9*	0.25*	8.65	351.2*	0.25*	24.09	268.4*
KM	0.50*	11.13	447.7*	0.50*	6.50	267.7*	0.50*	18.07	205.1*
N	1.00	246.	16.3	1.00	313.	21.8	1.00	284.	24.1
SZM									
U	-1.06	0.25		-1.27	0.08		-1.18	0.14	
V	-0.35	0.53		-0.56	0.66		-0.43	0.63	
W*	-0.15	0.21		-0.30	0.42		-0.37	0.44	
η	-0.14	0.35		-0.16	0.39		-0.16	0.40	
KH	0.25*	1.68	129.5*	0.25*	3.80	143.9*	0.25*	3.18	133.5*
KM	0.50*	1.18	98.1*	0.50*	2.69	108.5*	0.50*	2.22	101.2*
N	1.00	199.	23.3	1.00	186.	25.4	1.00	194.	25.5
SCRUM(MY)									
U	-1.11	0.04		-1.08	0.19		-1.02	0.14	
V	-0.30	0.37		-0.43	0.48		-0.60	0.55	
W*	-1.71	3.31		-2.90	3.63		-3.17	3.01	
η	-0.41	0.36		-0.18	0.40		-0.21	0.42	
KH	0.25*	1.00	45.10*	025*	0.86	46.63*	0.25*	0.83	47.20*
KM	0.50*	0.79	45.05*	0.50*	0.68	46.34*	0.50*	0.66	46.20*

*) Values are in the CGS unit system. W is ωh (POM and SZM) or ωh_z (SCRUM).

Tab. 2b. The Wind Driven Experiment: Upwelling

	30 d			60 d			90 d		
	Mn	Mx	Av	Mn	Mx	Av	Mn	Mx	Av
POM									
U	-0.64	0.86		-0.12	0.79		-0.19	1.10	
V	-0.38	0.29		-0.46	0.34		-0.70	0.39	
W*	-0.07	0.07		-0.09	0.08		-0.10	0.08	
η	-0.31	0.13		-0.32	0.16		-0.32	0.17	
KH	0.25*	17.59	220.7*	0.25*	6.45	159.5*	0.25*	4.83	109.5*
KH	0.50*	13.19	169.2*	0.50*	4.83	122.4*	0.50*	3.62	84.3*
N	1.00	214.	15.9	1.00	255.	19.5	1.00	373.	21.8
SZM									
U	-0.13	0.81		-0.27	0.67		-0.35	0.90	
V	-0.56	0.49		-0.53	0.34		-0.58	0.36	
W*	-0.22	0.24		-0.28	0.26		-0.33	0.35	
η	-0.25	0.12		-0.25	0.14		-0.25	0.15	
KH	0.25*	1.80	212.5*	0.25*	2.59	370.7*	0.25*	3.12	480.6*
KM	0.50*	2.11	156.2*	0.50*	3.60	266.9*	0.50*	4.37	343.8*
N	1.00	126.	19.5	1.00	118.	20.3	1.00	141.	20.9
SCRUM(MY)									
U	-0.32	1.07		-0.63	1.20		- 0.52	1.33	
V	-0.51	0.47		-0.85	0.77		- 1.03	0.96	
W*	-2.85	4.54		-7.01	12.45		-11.64	12.68	
η	-0.31	0.24		-0.60	0.52		- 0.78	0.81	
KH	0.25*	0.75	52.68*	0.25*	4.44	67.93*	0.25*	3.95	78.43*
KM	0.50*	0.65	51.25*	0.50*	3.54	63.74*	0.50*	3.18	72.23*

*) Values are in the CGS unit system.

LATERAL MIXING

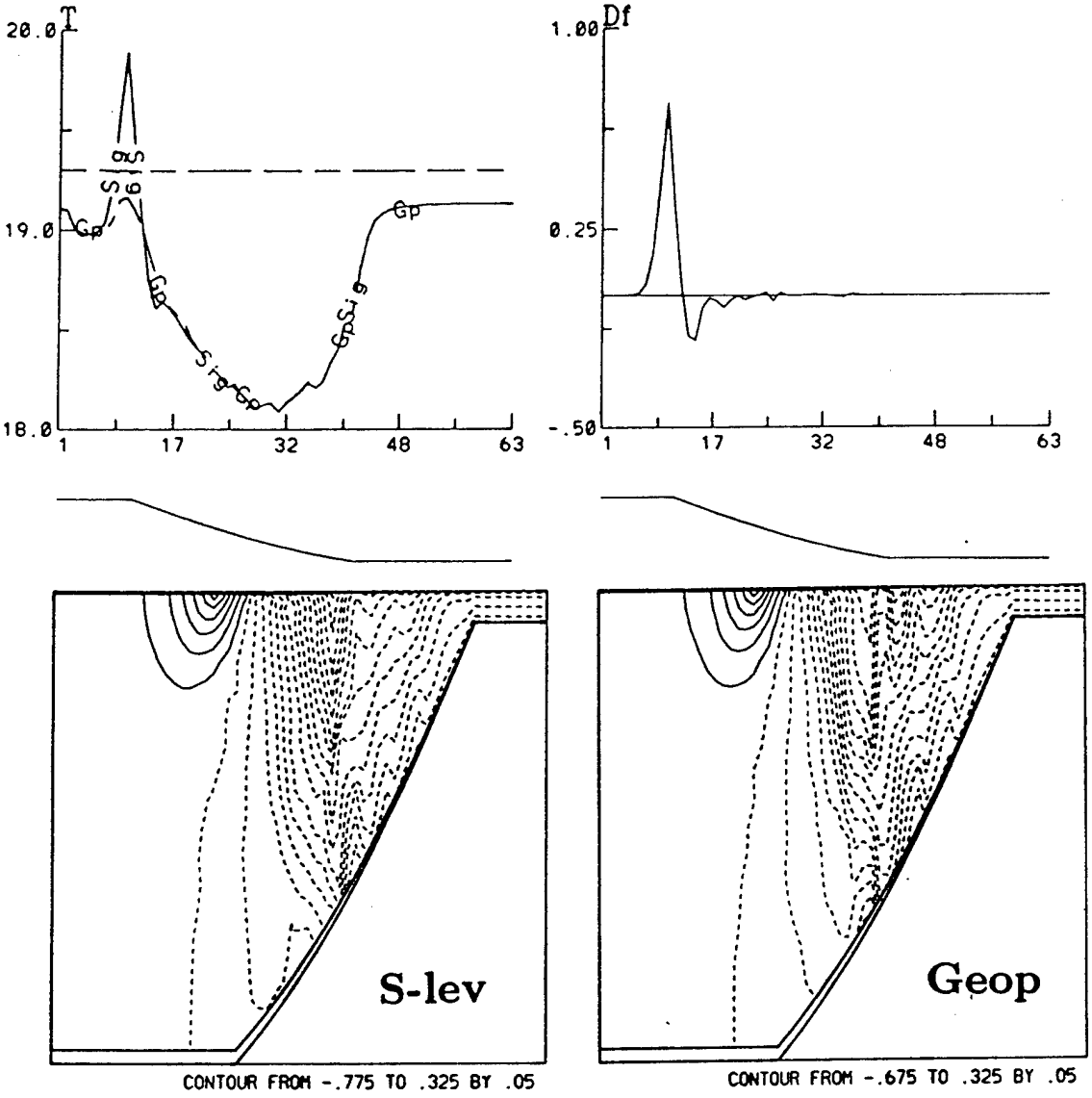

Fig. 1. Cross channel sea surface temperature from the σ-level and geopotential horizontal mixing algorithms (a). Sea surface temperature differences between the two solution (b). Along-shore coastal jet structure for the two lateral mixing formulations (c and d).

Coastal Front

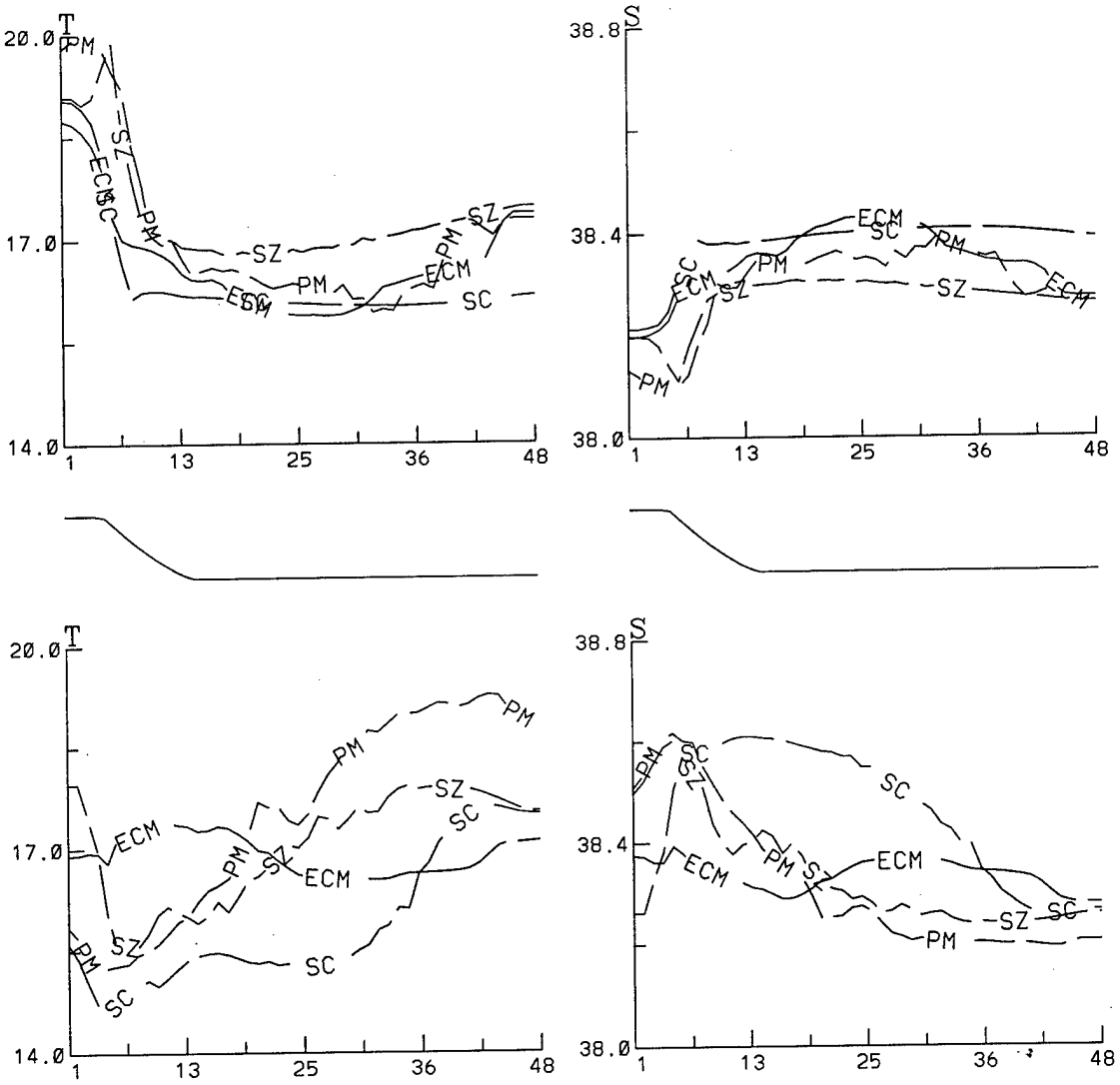

Figure 2

1-D PROBLEM

$\Delta x=4$

POM

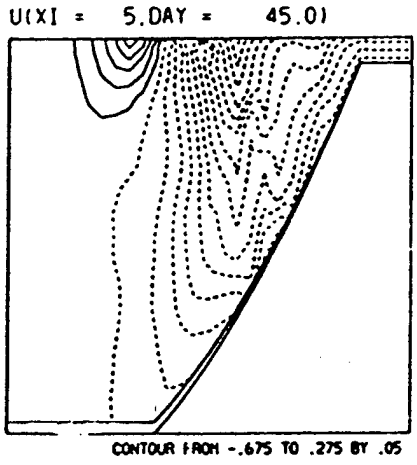

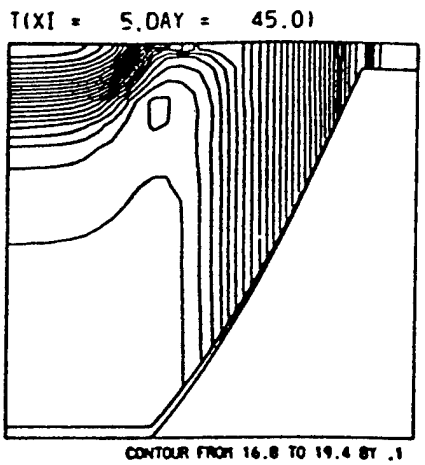

SCRUM

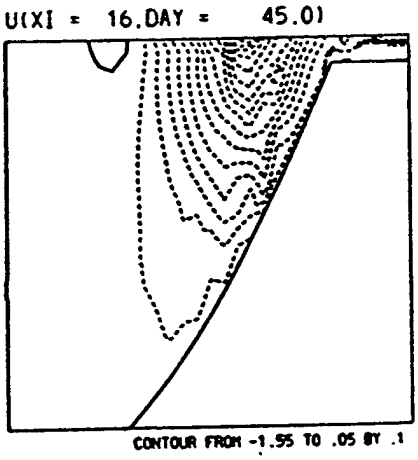

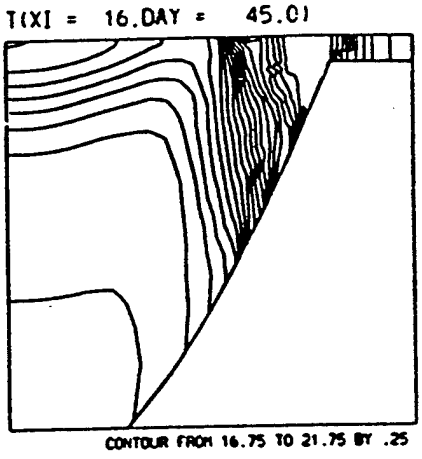

SZM

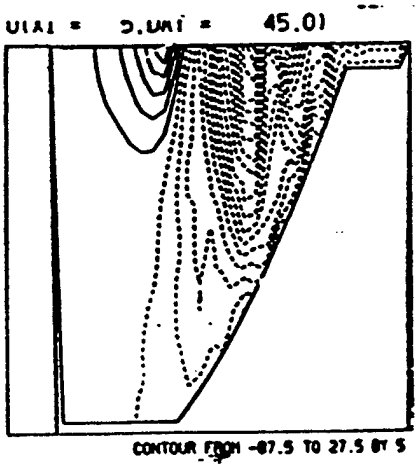

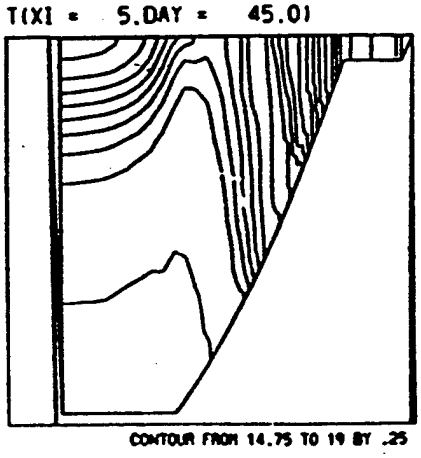

Figure 3a

1-D PROBLEM

$\Delta x=1$

POM

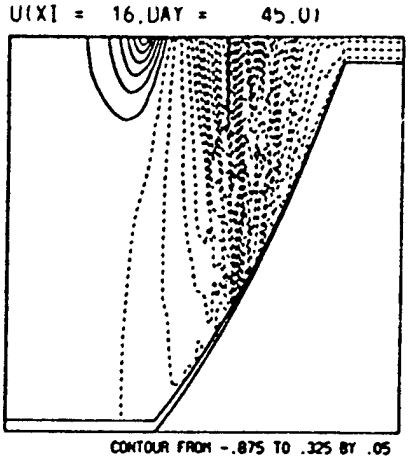

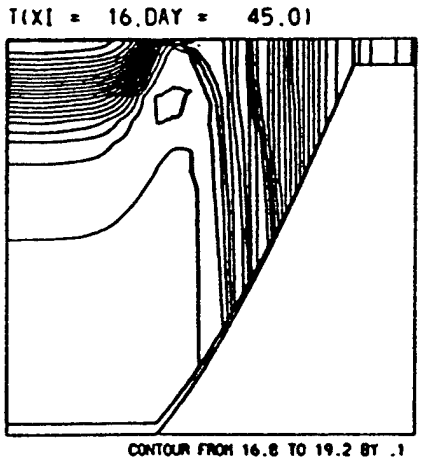

SCRUM

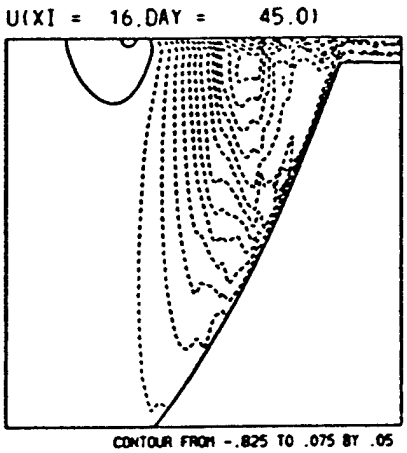

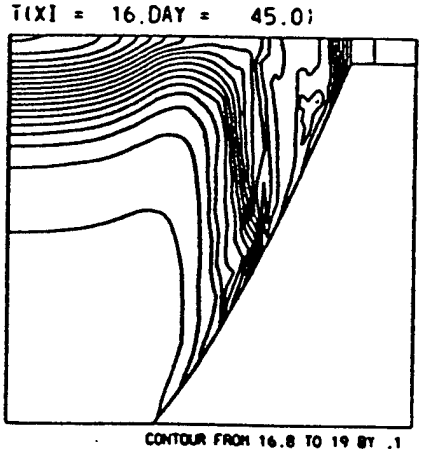

SZM

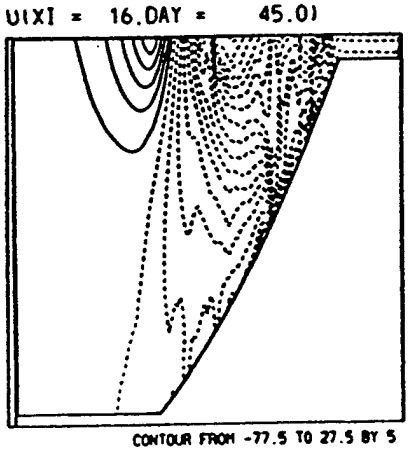

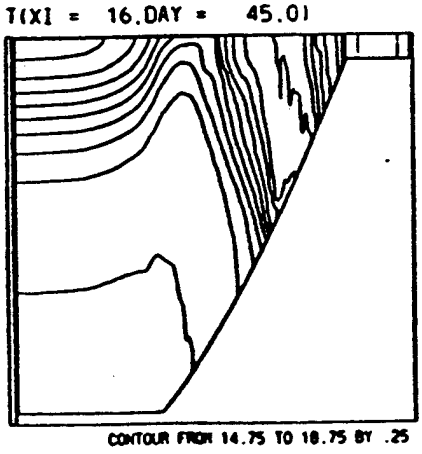

Figure 3b

POM V-vel Dx=2

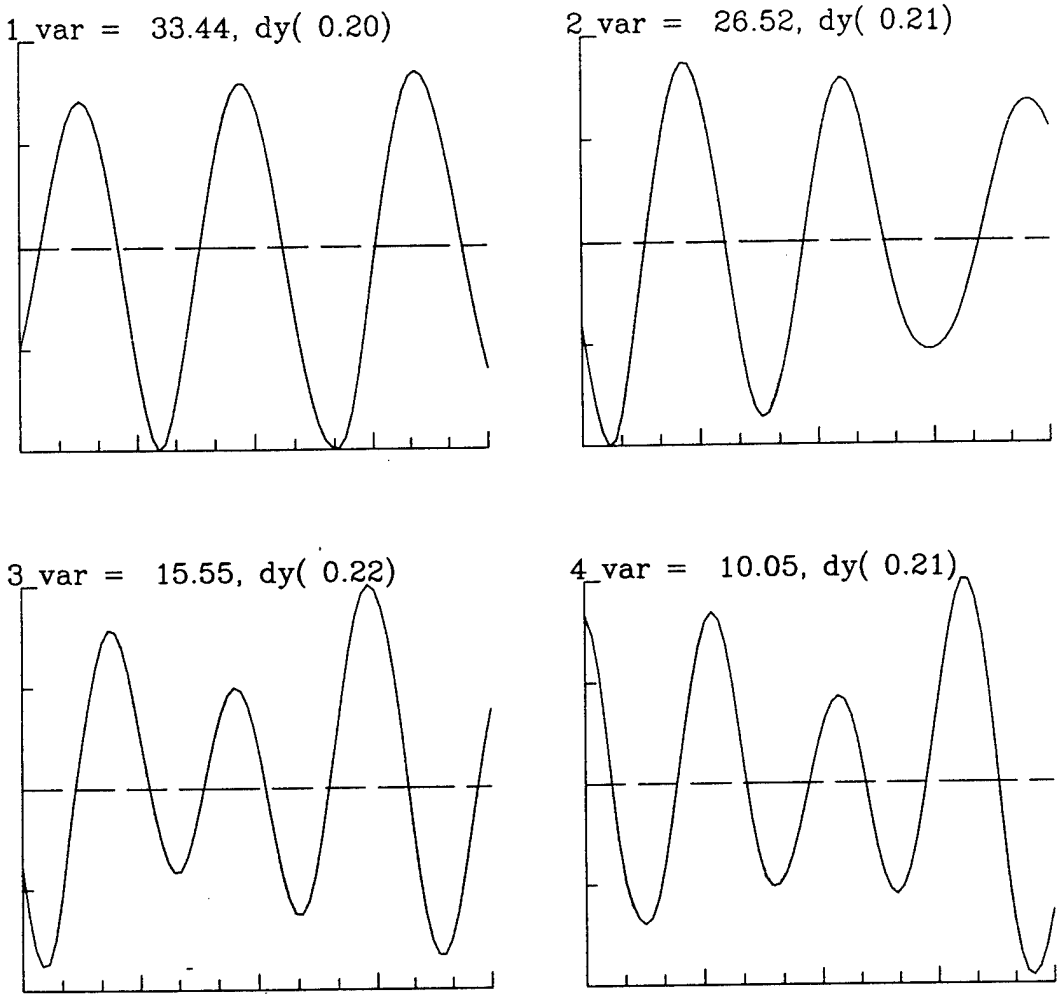

Figure 4a

SZM V-vel Dx=2

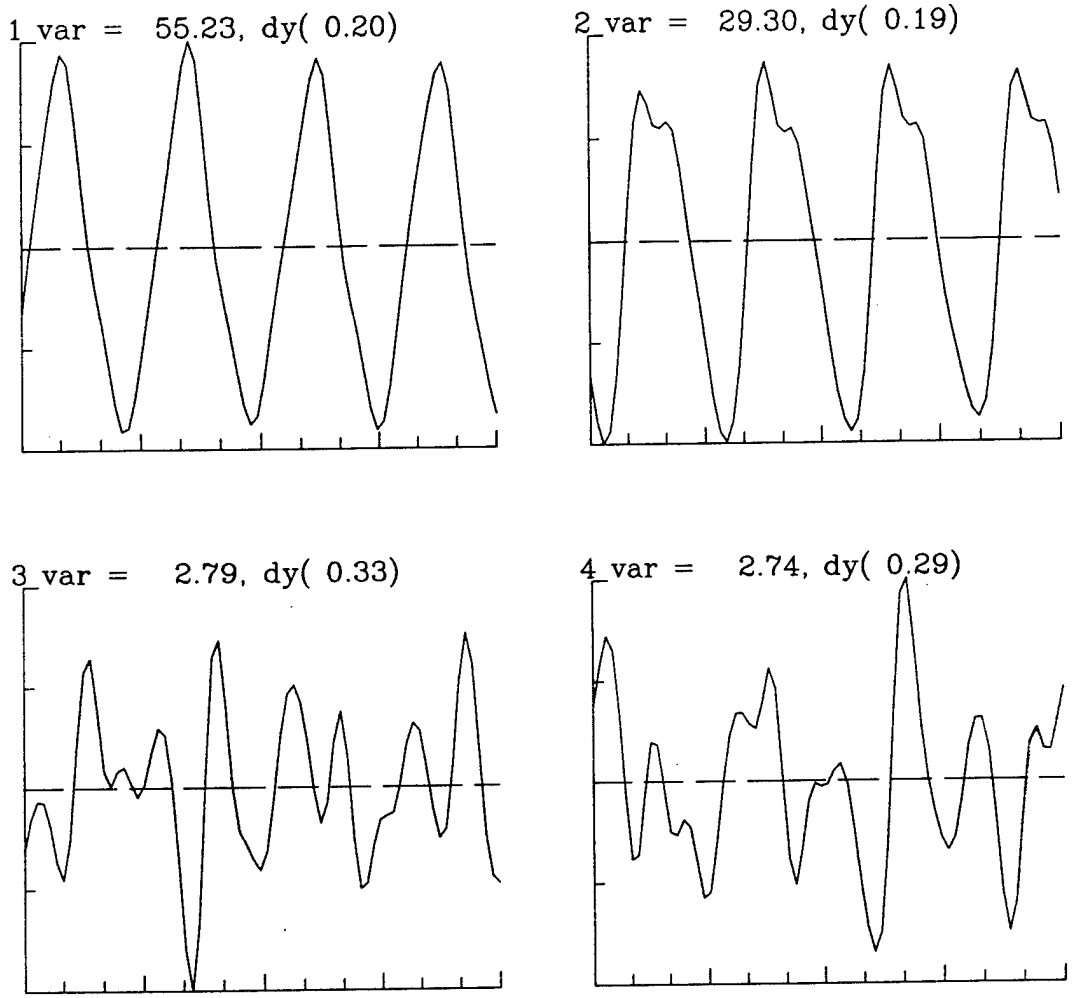

Figure 4b

SCR MY2.0 Vvel Dwn Dx=2

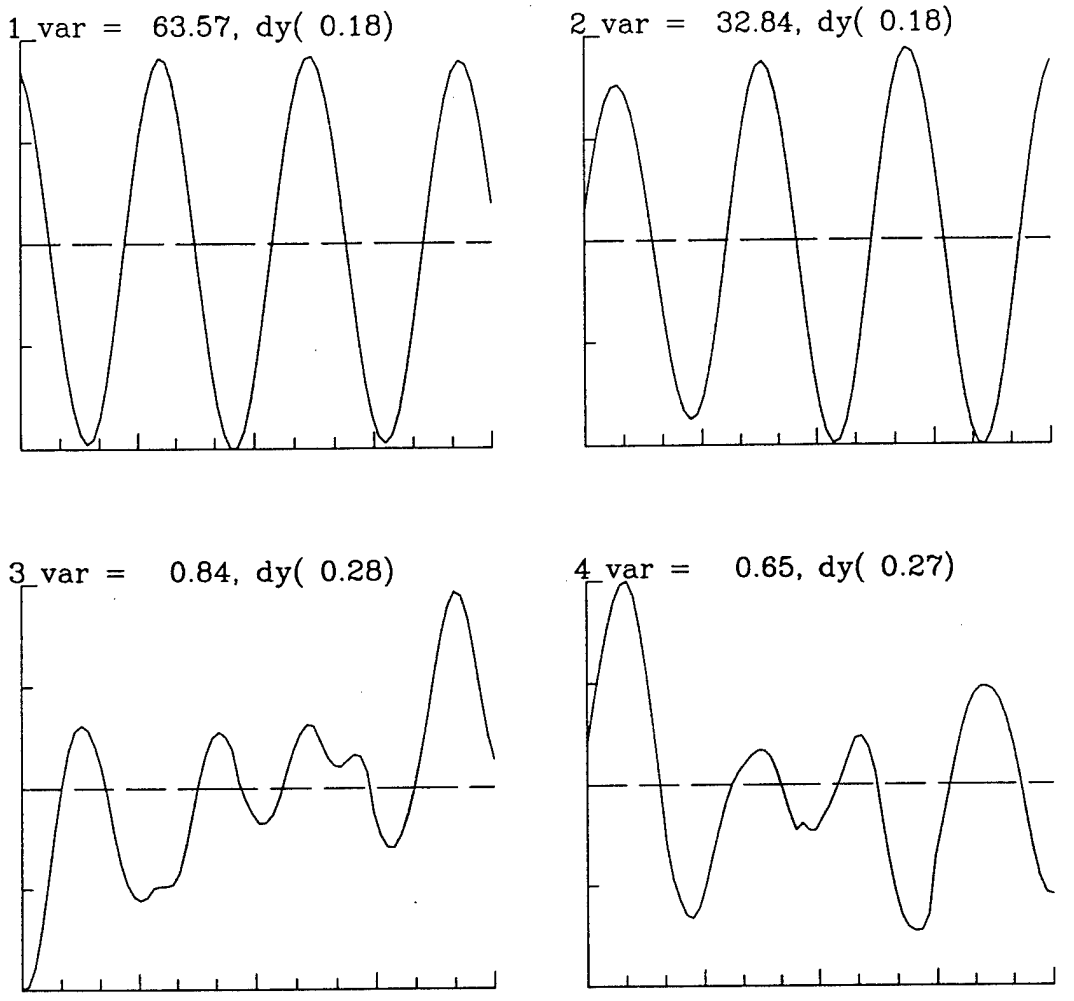

Figure 4c

POM Hour = 240

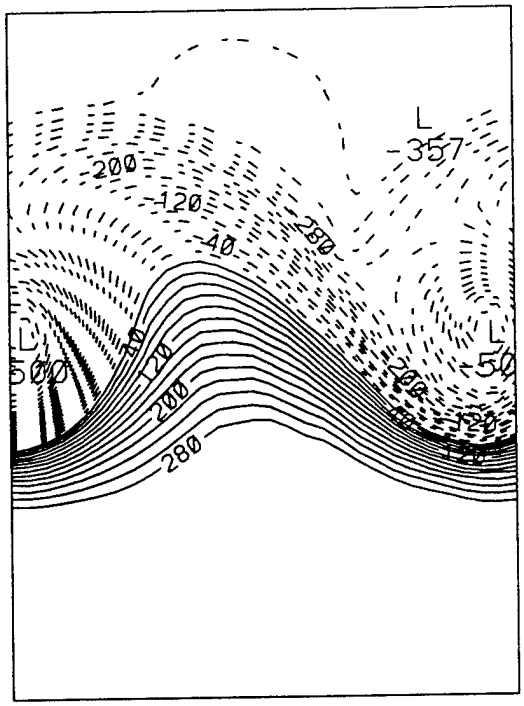

CONTOUR FROM -0.50018E-01 TO 0.27982E-01 CONTOUR INTERVAL OF 0.20000E-02 PT(3,3)= 0.37499E-01 LABELS SCALED BY 10000.

Figure 5a

SCRM Hour = 240

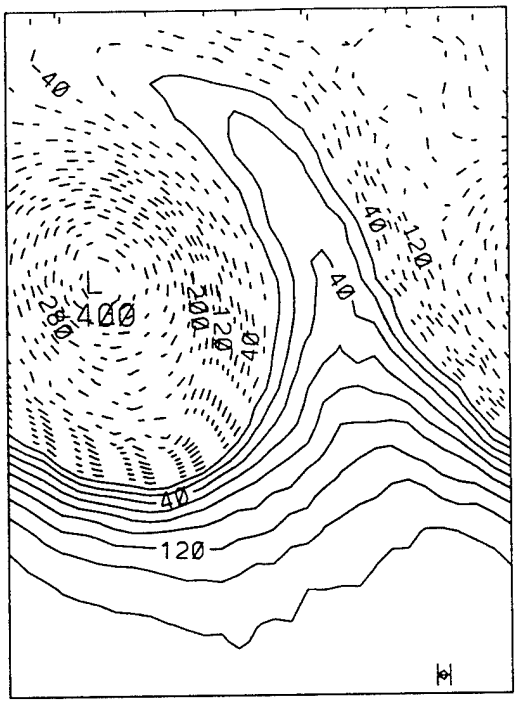

CONTOUR FROM -0.39957E-01 TO 0.18043E-01 CONTOUR INTERVAL OF 0.20000E-02 PT(3,3)= 0.17664E-01 LABELS SCALED BY 10000.

Figure 5b

SZM Hour = 237

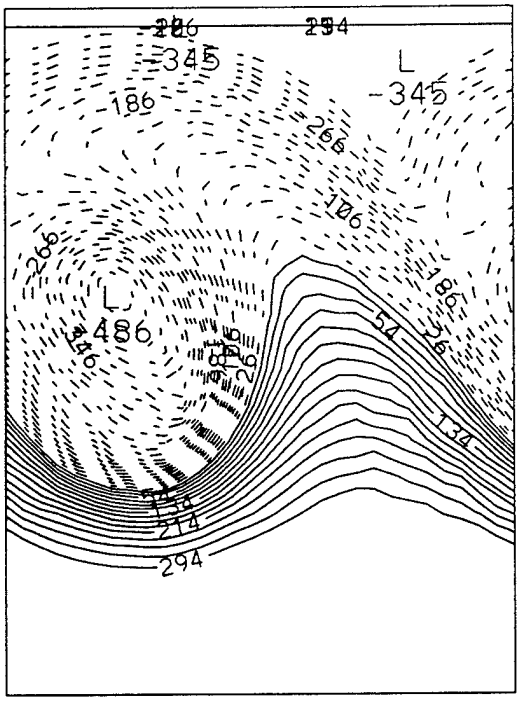

CONTOUR FROM -0.48648E-01 TO 0.29353E-01 CONTOUR INTERVAL OF 0.20000E-02 PT(3,3)= 0.38547E-01 LABELS SCALED BY 10000.

Figure 5c

REPORT DOCUMENTATION PAGE

Form Approved
OMB No. 0704-0188

1. Agency Use Only *(Leave blank).*	2. Report Date.	3. Report Type and Dates Covered.

4. Title and Subtitle.
Coastal Model Performance Evaluation and Comparison

5. Funding Numbers.
Program Element No.
Project No.
Task No.
Accession No.

6. Author(s).
Germana Peggion

7. Performing Organization Name(s) and Address(es).
The University of Southern Mississippi
Institute of Marine Sciences
Building 1103 Room 249
Stennis Space Center, MS 39529

8. Performing Organization Report Number.

9. Sponsoring/Monitoring Agency Name(s) and Address(es).
Office of Naval Research
Code 252: AAT
Ballston Tower One
800 North Quincy Street
Arlington, VA 22217-5660

10. Sponsoring/Monitoring Agency Report Number.

11. Supplementary Notes.
ONR Research Grant No. N00014-95-1-0181

12a. Distribution/Availability Statement.
Approved for public release; distribution unlimited.

12b. Distribution Code.

13. Abstract *(Maximum 200 words).*

This study compares several ocean circulation models in coastal applications. The comparison is restricted to 3-D, primitive equation, free-surface models on sigma-like vertical coordinate systems. The models differ in their treatment of the barotropic flow, horizontal and vertical mixing, temporal and spatial differencing, and other details. The physical accuracy and the numerical character of the models are evaluated and discussed on a variety of test problems. The coastal study processes include wave propagation, upwelling and downwelling regimes, and genesis and evolution of fronts.

The study indicates that the solutions may sensibly differ from model to model. This is primarily due to: 1) different response to the calibration of the physical and numerical parameters, 2) peturbations in the dynamical balances. In general, differences in the primary features (such as front location, strength of the coastal jet) can be adjusted by adequate calibrations. Representation of the secondary features (such as internal wave propagaiion, temperature and salinity anomalies) may depend upon different parameterizations and numerical treatments of the same physical terms that may alter the relative importance of the dominant processes.

14. Subject Terms.
(U) Coastal applications, (U) Limited-area models, (U) Ocean models, (U) Ocean model comparison, (U) Ocean model evaluation

15. Number of Pages.
29

16. Price Code.

17. Security Classification of Report.	18. Security Classification of This Page.	19. Security Classification of Abstract.	20. Limitation of Abstract.
UNCLASSIFIED	UNCLASSIFIED	UNCLASSIFIED	SAR